Nano- and Microgels of Poly(Vinyl Methyl Ether) Obtained by Radiation Techniques

Janusz M. Rosiak*

Institute of Applied Radiation Chemistry, Technical University of Lodz,
Wroblewskiego St. 15, 93-590 Lodz, Poland

Abstract

Hydroxyl radicals were generated radiolytically in N_2O-saturated aqueous solutions in the presence of poly(vinyl methyl ether) (PVME, 6×10^4 Da, 10^{-3}-10^{-2} mol·dm^{-3} in monomer units). As measured by pulse radiolysis, they react ($k = 2.2\times10^8$ dm^3·mol^{-1}·s^{-1}) with PVME by giving mainly rise to α-alkoxyalkyl radicals (~72%) that reduce ($k \approx 2\times10^9$ dm^3·mol^{-1}·s^{-1}) Fe(CN)$_6^{3-}$, IrCl$_6^{2-}$ or tetranitromethane. Based on the formaldehyde yield in the presence of the latter two oxidants (~40% of $^\bullet$OH), it is concluded that OH radicals undergo H-abstraction at ROCH$_2$–H, R$_3$C–H and R$_2$HC–H with probabilities of ~40%, ~32% and ~28%, respectively. The momentary rate constant of the decay of the PVME radicals depends on the number of radicals per polymer chain and drops as they decay. The yield of intermolecular crosslinks, as measured by an increase of the molecular weight, strongly increases with decreasing dose rate, and it is concluded that the majority of crosslinks occur intramolecularly, even at the lowest dose rate used (0.0015 Gy·s^{-1}, G(intermolecular crosslinks) = 0.62×10^{-7} mol·J^{-1}).

At low temperatures and low polymer concentrations the intramolecular crosslinking reaction is favored. A large number of radicals are formed in a short period of time during each pulse of accelerated electrons. The combination of the formed polymeric radicals is in the intramolecular way and nanogels formation occurs. Without changes in the molecular weight the dimension (radius of gyration and hydrodynamic radius), as well as the intrinsic viscosity of the nanogels decreases with increasing radiation dose. At temperatures above the LCST PVME molecules collapse to globular particles. Electron beam irradiation of these stable phase-separated structures leads to the formation of temperature-sensitive microgel particles. The additive-free method of crosslinking of polymers in aqueous solutions by high-energy radiation offers the application of these microgels in the field of medicine because of no remaining toxic substances (monomers, initiators, crosslinkers, *etc.*). The variation of the crosslinking density and the particle diameter can be performed by varying the polymer concentration and the radiation dose. Applying the closed-loop system reduces the amount of un-crosslinked molecules (sol content).

Introduction

Poly(vinyl methyl ether), PVME, is one of the simplest water-soluble polymers (for its synthesis and solution properties see ref. [1]). Its aqueous solutions have the unusual property of reverse temperature solubility, *i.e.* the polymer precipitates at around 34-37°C. Its interactions with water and the mechanism of the phase transitions are presently the subject of considerable interest [2-4].

Hydrogels, *i.e.* water-swollen, covalently crosslinked polymer networks, made of poly(vinyl methyl ether) are also heat-sensitive [5-8]. This property, as well as the fact that the gel collapses at a temperature close to body temperature, has elicited a number of studies on its possible use as a stimulus-sensitive biomaterial, *e.g.* as a thermosensitive (and/or bioadhesive) drug-delivery system [7,9-11] and even as an artificial muscle [7,12]. Other interesting applications of poly(vinyl methyl ether) hydrogels are recyclable separation systems [5,13,14] and chemomechanical valves [15].

In general, ionizing radiation is a very efficient tool for the formation of hydrogels [16]. The reaction can be carried out at room temperature, is easy to control and environment-friendly (no additional chemicals, no waste). Using γ-irradiation, homogeneous products of any desired shape and size can be pro-

---

*corresponding author. E-mail: http://mitr.p.lodz.pl/biomat

duced. For biomedical applications, the radiation technique allows one to carry out in one step the formation of the hydrogel as well as its sterilization (*e.g.* refs. [17,18]).

In particular, hydrogels of poly(vinyl methyl ether) have already been obtained by this method [6,8,19-21]. For a further development of this promising technique, it seems worthwhile to investigate in some detail the underlying radiation chemistry of poly(vinyl methyl ether) in aqueous solution. First attempts in elucidating these processes have already been undertaken [20-22], but there are marked discrepancies among the published data.

The aim of the present work is to present a more complete picture by combining kinetic and product studies. To aid our interpretations, the radiation-induced reactions of 2,4-dimethoxypentane, a low-molecular-weight model compound of poly(vinyl methyl ether), were also investigated and are described in the preceding paper [23].

Experimental

Poly(vinyl methyl ether) (Lutonal M40, BASF) has been purified by dissolving it in water (~50 g·dm^{-3}) at room temperature. The temperature of solution was then raised above 37°C until the polymer precipitated. The liquid fraction was discarded, and after this procedure had been repeated five times the polymer solution was subjected to continuous ultrafiltration (Amicon TCF 10 with a Diaflo YM10 membrane of a nominal 10 kDa cut-off) until the UV absorption $\lambda > 200$ nm of the permeate fell below 0.01. After such a treatment the weight-average molecular weight of PVME was 6×10^4 Da as determined by low-angle laser light-scattering.

Tetranitromethane was washed several times with water to reduce the background level of nitroform anion. All other chemicals were of analytical grade. Solutions were made-up in Milli-Q-filtered (Millipore) water.
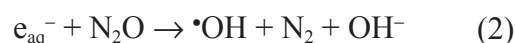
γ-Irradiations were carried out with a panorama ^{60}Co-γ-source (Nuclear Engineering) at dose rates ranging from 0.0015 to 0.15 Gy·s^{-1}. Pulse radiolysis experiments were performed with a 2.8 MeV van de Graaff accelerator generating electron pulses of 0.4 μs duration, equipped with optical and conductometric detection systems [24]. Optical measurements were based on thiocyanate dosimetry [25] and conductometric measurements on dimethyl sulfoxide dosimetry [26].

Formaldehyde was determined by HPLC after derivatization with 2,4-dinitrophenyl-hydrazine (Nucleosil C18 column, eluent: acetonitrile-water 1/1 v/v, optical detection at $\lambda = 360$ nm) [27]. The yield of H_2O_2 and organic hydroperoxides was determined spectrophotometrically with molybdate-activated iodide [28]. The absorbance of I_3^- resulting from the reaction with H_2O_2 appears immediately after mixing, while the subsequent slower increase is attributed to the reduction of organic hydroperoxides (*cf.* ref. [29]).

The weight-average molecular weight was determined by low-angle laser light-scattering at $\lambda = 633$ nm (Chromatix KMX-6) after having filtered the samples (0.45 μm, Minisart NML, Millipore). The specific refractive index increment (dn/dc) of PVME in aqueous solutions was determined with a laser differential refractometer (Chromatix KMX-16, $\lambda = 633$ nm, 25°C). Extrapolation to zero PVME concentration yielded dn/d$c = 0.127$ cm^3·g^{-1}. Molar concentrations of PVME solutions are given in terms of its repeating unit (molecular weight = 58 g·mol^{-1}).
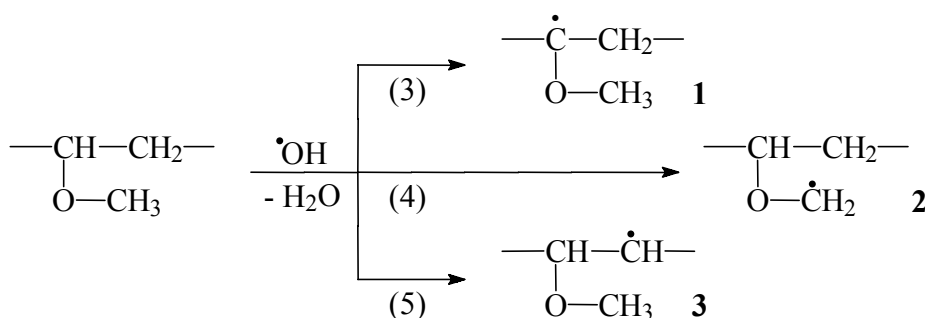
Generation and UV-optical properties of PVME radicals

Upon irradiation of dilute, N$_2$O-saturated PVME solutions, OH radicals and H atoms are formed in reactions (1) and (2). Under such conditions the radiation-chemical yield of OH radical is $G = 5.8\times10^{-7}$ mol·J^{-1}, while the H atoms are formed with $G = 0.6\times10^{-7}$ mol·J^{-1}.

$$H_2O \xrightarrow[\text{radiation}]{\text{ionizing}} e_{aq}^-, {}^\bullet OH, H^\bullet, H^+, H_2O_2, H_2 \quad (1)$$

$$e_{aq}^- + N_2O \rightarrow {}^\bullet OH + N_2 + OH^- \qquad (2)$$

The OH radicals and H atoms react with PVME by H-abstraction [*e.g.* reactions (3)-(5)]. For the sample used in present study, the rate constant for the OH radical is 2.2×10^8 dm^3·mol^{-1}·s^{-1} [22], while the H atoms react more slowly ($k < 1\times10^7$ dm^3·mol^{-1}·s^{-1}) [21,22].

Initial absorption spectra of PVME-radicals 1-3 are featureless and only show an increasing absorbance towards shorter wavelength [22]. Thus, they resemble the spectra of the radicals derived from the model compound 2,4-dimethoxypentane [23] as well as spectra for other ether-derived radicals, *e.g.* diisopropyl ether [30] and 2,4-dioxane [31]. It has been reported that the absorption spectra of PVME-derived radicals maximize at 310 nm [20]. We reproduced this result with a non-purified commercial sample,

$$
\begin{array}{c}
\underset{\overset{|}{O-CH_3}}{-CH-CH_2-} \quad \underset{-H_2O}{\overset{\bullet OH}{}}
\end{array}
$$

(3) → $-\overset{\bullet}{\underset{\overset{|}{O-CH_3}}{C}}-CH_2-$ **1**

(4) → $-\underset{\overset{|}{O-\overset{\bullet}{C}H_2}}{CH-CH_2-}$ **2**

(5) → $-\underset{\overset{|}{O-CH_3}}{CH-\overset{\bullet}{C}H-}$ **3**

and conclude that low-molecular-weight impurities contained in the commercial material must give rise to the absorption maximum at 310 nm.

Oxidation of radicals 1 and 2 by $Fe(CN)_6^{3-}$, $IrCl_6^{2-}$ and tetranitromethane

Among the three radicals which are formed upon $\bullet OH$ attack [reactions (3)-(5)] radicals 1 and 2 carry an alkoxyl group in α-position and thus are strongly reducing, i.e. they react rapidly with oxidants. Their one-electron oxidation leads to carbocations [e.g. 4, reaction (6)] which react rapidly with water giving rise to hemiacetals [e.g. 5, reaction (7)]. These are unstable and, for example, 5 releases formaldehyde [reaction (8)].

In a pulse radiolysis experiment, the oxidation by $Fe(CN)_6^{3-}$ has been studied by following the bleaching of $Fe(CN)_6^{3-}$ at $\lambda = 420$ nm as a function of the $Fe(CN)_6^{3-}$ concentration. There was only one kinetic component in the bleaching process ($k = 1.9 \times 10^9 \, dm^3 \cdot mol^{-1} \cdot s^{-1}$), and the total bleaching of $Fe(CN)_6^{3-}$ corresponds to 75% of the initial yield of $\bullet OH + H^\bullet$. Thus, radicals 1 and 2 react at a very similar rate. At the low rate of the reaction of $H^\bullet$ with the polymer and its high rate with $Fe(CN)_6^{3-}$ ($k = 6.3 \times 10^9 \, dm^3 \cdot mol^{-1} \cdot s^{-1}$ [32]) practically all $H^\bullet$ (> 90%) is scavenged by $Fe(CN)_6^{3-}$. Based on this correction, we calculate that $\bullet OH$ radicals produce ~72% reducing radicals 1 and 2 and thus ~28% radicals 3.
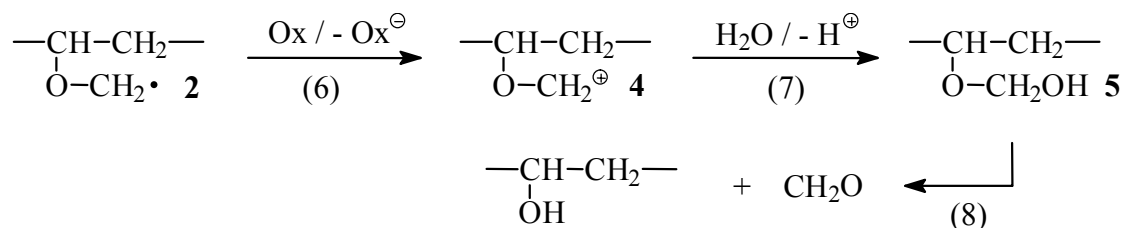
The same result was obtained upon γ-radiolysis. This indicates that an H-transfer reaction, that would convert radicals 3 into radicals 1 and/or 2 does not occur under these conditions. Such an H-transfer was,

in fact, observed in the free radical chemistry of low molecular alcohols [33] as well as in poly(vinyl alcohol) [34], where the rate constants for this reaction is in the order of 500 s^{-1}.

A similar phenomenon, as in PVME, i.e. the absence of a reasonably fast H-transfer, has also been observed with its low-molecular-weight model, 2,4-dimethoxypentane [23]. In H-transfer reactions, six-membered transition states are favourable, but five-membered transition states are not, i.e. in the latter case such reactions may be substantially retarded by steric effects. These seem to play a substantial role in PVME (an apparently also in the model system). In PVME, the polymer segments within the coil are packed much more tightly as in other polymers as evidenced by comparatively smaller coil dimensions at a similar molecular weight (Janik, unpublished results). This may suggest that there are structure-building hydrophobic interactions, which could also result in a high activation barrier for a configuration change necessary for the H-transfer.

In experiments carried out with other oxidants, namely tetranitromethane and $IrCl_6^{2-}$, the total yield of α-alkoxyalkyl radicals was confirmed, by optical measurements of nitroform anion formation and $IrCl_6^{2-}$ bleaching, to be ~75% of the initial yield of $\bullet OH + H^\bullet$, again, with no difference whether these experiments were carried out using pulse radiolysis or γ-radiolysis.

The oxidation of radicals 1 and 2 by tetranitromethane was also studied by pulse radiolysis with optical and conductometric detection. The use of the latter technique allowed us to monitor the release of protons. The rate of the reaction with tetranitrome-

$$-\underset{\overset{|}{O-CH_2\bullet}}{CH-CH_2-} \quad \underset{(6)}{\overset{Ox/-Ox^\ominus}{\longrightarrow}} \quad -\underset{\overset{|}{O-CH_2^\oplus}}{CH-CH_2-} \quad \underset{(7)}{\overset{H_2O/-H^\oplus}{\longrightarrow}} \quad -\underset{\overset{|}{O-CH_2OH}}{CH-CH_2-}$$
2   **4**   **5**

$$-\underset{\overset{|}{OH}}{CH-CH_2-} \quad + \quad CH_2O \quad \overset{}{\underset{(8)}{\longleftarrow}}$$

thane with 1 and 2 is $\sim 2 \times 10^9$ dm³·mol⁻¹·s⁻¹, as has also been observed for other α alkoxyl radicals [35]. First a short-lived adduct may be formed [*e.g.* 6, reaction (9)] which subsequently hydrolyses [reaction (10)] yielding the carbocation and nitroform anion which has been detected by its strong absorption at 350 nm. The carbocation is also very short-lived and a proton is released [*cf.* reaction (7)] which leads to the observed conductivity increase.

Decomposition of hemiacetal 5 leads to the formation of formaldehyde [reaction (8)] (analogous reaction was observed for the model compound, ref. [23]). The formaldehyde yield in the presence of the oxidants tetranitromethane or $IrCl_6^{2-}$, a measure of the yield of radicals 2, is $G = 2.4 \times 10^{-7}$ mol·J⁻¹, *i.e.* ~40% of initial yield of •OH [using $Fe(CN)_6^{3-}$ gives rise to only $G(CH_2O) = 1.3 \times 10^{-7}$ mol·J⁻¹; much lower $G(CH_2O)$ have also been observed for the radicals derived from 2,4-dimethoxypentane and dimethyl ether [23], *i.e.* side reactions must occur with this oxidant. Having established the yield of radical 2 at ~40% and the sum of 1 + 2 at ~72%, the yield of radical 1 is calculated at ~32%, and the remaining ~28% then must be attributed to radical 3. Based on the number of hydrogen atoms available for abstraction (random H-abstraction) one calculates 17% 1, 50% 2 and 33% 3. Thus there seems to be some preference for the formation of the tertiary radical 1. On the other hand, the formation of the primary radical 2, although stabilized by an alkoxyl group, seems not much favoured over that of the secondary radical 3. A substantial preference for abstraction of the tertiary hydrogen has also been noted in our model compound 2,4-dimethoxypentane (35% *vs.* 12.5% for random attack) [23] or diisopropyl ether (78% *vs.* 14% for random attack) [30].

Previously, data have been reported where the yield of radicals 1 plus 2 have been determined at only 26% by following their oxidation by thionine [20,21]. However, repeating this experiment with our purified sample led to a yield of about 70%, in good agreement with the value obtained with the other oxidants. Here, the error might have arisen from the high scavenging capacity of low-molecular-weight contaminations (*cf.* also spectral differences). We

therefore believe that the values reported previously [20,21] are on the low side.

We also have to correct our own preliminary data, where the yield of radicals 1 plus 2 was estimated at ~54% [22]. There were probably two sources for errors that may have contributed to this underestimate; a different (and probably less efficient) purification technique, and dosimetry problems due to a relatively poor long-time stability of the electron beam parameters when the ELU-6 linear accelerator (a machine different from the one used in the present study) was operated in the untypical low dose mode.
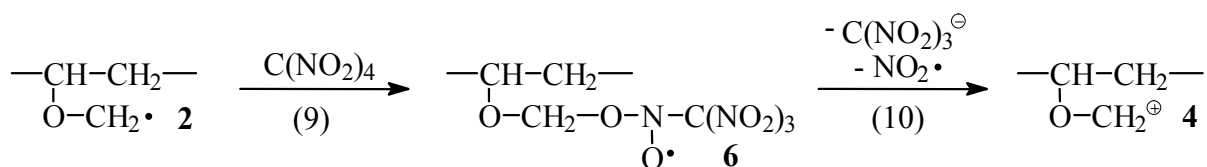
Decay of the PVME radicals

The radicals derived from the PVME model compound 2,4-dimethoxypentane decay with an overall bimolecular rate constant of $2k = 1 \times 10^9$ dm³·mol⁻¹·s⁻¹ [23]. In contrast, the bimolecular decay of PVME radicals cannot be described by simple second-order kinetics (*cf.* also ref. [20]). Similar effects have been described for a number of other polymers and their low-molecular-weight models [36-40].

When the reciprocal of the radical concentration ([R•]) is plotted *vs.* the time, a straight line is obtained if simple second-order kinetics are followed. For PVME, however, such a plot is strongly curved (Fig. 1), and the observed momentary second-order rate constant decreases with time.

Bimolecular rate constants calculated from the slopes of curves of the type shown in Fig. 1 (main graph) are shown in the inset as a function of the average number of radicals present on each polymer chain (Z_R). The three data sets represent different irradiation conditions (dose per pulse and polymer concentration), *i.e.* three different initial average numbers of radicals per chain Z_{R_0}. The polymer concentrations in our experiments are lower than the critical hydrodynamic concentration (for our sample ~0.5 mol·dm⁻³ at 25°C as estimated by viscometry and multi-angle laser light-scattering); *i.e.* the polymer coils do not overlap.

For understanding why the momentary termination rate constant decreases in the course of the reaction, one has to recall that in pulse radiolysis many radicals are formed at each macromolecule. This im-
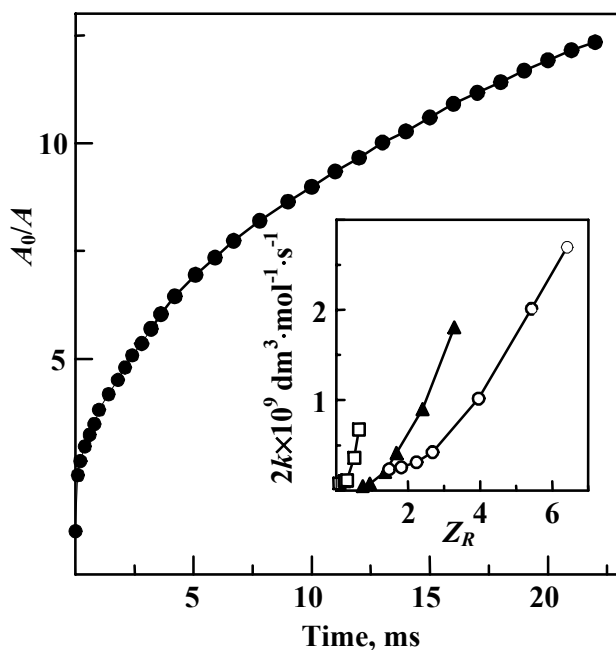
$$\underset{\overset{|}{O-CH_2\cdot}\ \ \mathbf{2}}{-CH-CH_2-} \xrightarrow[\ (9)\ ]{C(NO_2)_4} \underset{\overset{|}{O-CH_2-O-\underset{\overset{|}{O\cdot}\ \ \mathbf{6}}{N}-C(NO_2)_3}}{-CH-CH_2-} \xrightarrow[\ (10)\ ]{\overset{\displaystyle -C(NO_2)_3^{\ominus}}{-NO_2\cdot}} \underset{\overset{|}{O-CH_2^{\oplus}}\ \ \mathbf{4}}{-CH-CH_2-}$$

Fig. 1. Pulse radiolysis of PVME (1×10^{-3} mol·dm^{-3}) in N$_2$O saturated aqueous solution. The ratio of the absorbance at 290 nm directly after pulse (A_0) to the absorbance (A) observed at a given time after the pulse. Inset: momentary second-order rate constants as a function of concentration of radicals per macromolecule Z_R. Polymer concentration: 2×10^{-3} mol·dm^{-3} (O), 1×10^{-2} mol·dm^{-3} (▲) and 1×10^{-1} mol·dm^{-3} (□).

plies that, at least in the first stages, recombination is mainly intramolecular. Radicals at a polymer chain cannot move freely and independently, as in homogeneous, diffusion-controlled reactions. Instead, a distribution of distances and possibly of activation energy exists, which implies different reactivities. Moreover, in the course of termination new C–C bonds are formed between the segments. This decreases segment mobility, and slows down the rate of the subsequent termination event. Two more sources of deviation from the homogeneous kinetics may be mentioned. The initial spatial distribution of the radicals within the macromolecule is not random, but rather reflects the fact that •OH radicals are formed in spurs. Those radicals formed in a close vicinity are expected to recombine fast. At a later stage, when the average Z_R is close to one, many macromolecules bear only one radical. These radicals have to terminate intermolecularly, *i.e.* the termination mechanism now changes. In addition to segmental diffusions, intermolecular termination requires the diffusion of macromolecules as a whole, and therefore is slower than the intramolecular termination.

When the three data sets in the inset of Fig. 1 are compared, it becomes evident that the momentary rate constant of termination depends not only on the momentary number of radicals per chain Z_R, but also on the initial number of radicals per chain, Z_{R_0}. In fact, when we compare data for equal Z_R but different Z_{R_0}, we compare recombination at different stages. A sample which starts with a low Z_{R_0} is at a relatively early stage, *i.e.* it has only some radical pairs for recombination and no or only a few internal crosslinks. On the other hand, a sample which starts with a high Z_{R_0} is, at the same Z_R, at a later stage, with no more fast-reacting pairs and a higher number of internal crosslinks. As a consequence of this, the momentary termination rate constant, if compared for two samples of the same Z_R, is lower for the sample of higher Z_{R_0}.

Crosslinking of PVME chains

Under dioxygen-free conditions, the resulting molecular weight depends on the ratio of the rate constants of radical recombination and chain scission. Unimolecular chain scission resulting from β-fragmentation of polymer radicals is typically a slow process [*e.g.* for poly(acrylic acid) $k = 0.025$ s^{-1} [39], for poly(methacrylic acid) [41,42] $k = 1.8$ s^{-1}] and only plays a role when the competing recombination reactions are slow as well. This is especially the case with radicals derived from polyelectrolytes such as poly(acrylic acid) and poly(methacrylic acid), where, due to the repulsive electrostatic forces between the charged chains, the termination rate constants are <100 dm^3·mol^{-1}·s^{-1} [39,41-43]. With the exception of polysaccharides [44], for the irradiation of uncharged polymers, where the termination rate constants are typically in the order of 10^7-10^9 dm^3·mol^{-1}·s^{-1}, no decrease in the molecular weight of the polymer has been reported.

When termination dominates over scission, the extent of the increase in average molecular weight depends on two more factors: the proportion between recombination and disproportionation and the ratio between inter- and intramolecular recombination.

The data on the model compound, 2,4-dimethoxypentane, indicate that β-fragmentation reactions must be of little importance and that recombination and disproportionation occur with equal probability [23]. Thus, one may expect that chain scission is also negligible in the case of PVME. Assuming a similar ratio of recombination to disproportionation would

thus set the total (intra- plus intermolecular) crosslinking yield close to 1.5×10^{-7} mol·J^{-1}.

The increase in weight-average molecular weight of PVME upon γ-irradiation in N$_2$O-saturated solutions is shown in Fig. 2.
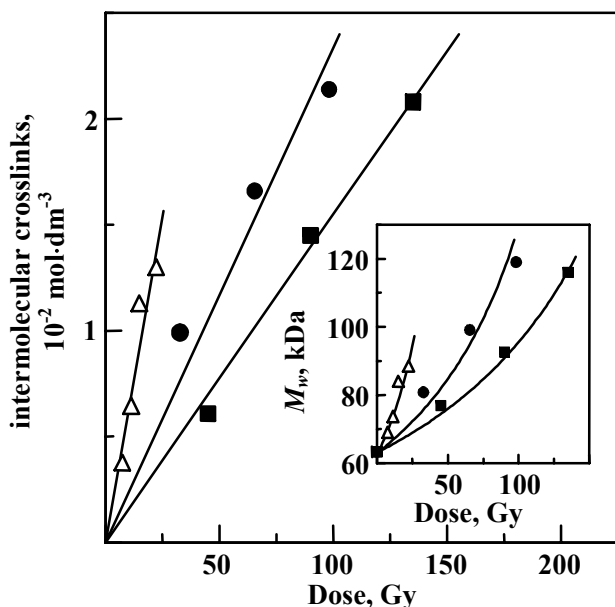

Fig. 2. γ-Radiolysis of PVME (1×10^{-2} mol·dm^{-3}) in N$_2$O-saturated aqueous solutions. Concentration of intermolecular crosslinks (main graph) and weight-average molecular weight (inset) as a function of dose. Dose rates: 0.15 Gy·s^{-1} (●), 0.013 Gy·s^{-1} (■) and 0.0015 Gy·s^{-1} (△).

Based on equation (3) [45,46], where M_{w_0}, M_w (in g·mol^{-1}) are the weight-average molecular weights before and after irradiation and c_{PVME} is the polymer concentration (in g·dm^{-3}), the concentration of intermolecular crosslinks was calculated.

$$[\text{intermolecular crosslinks}] =$$
$$= 0.5 \times (M_{w_0}^{-1} - M_w^{-1}) \times c_{PVME} \qquad (3)$$

The linear plots of the concentration of intermolecular crosslinks *vs.* the dose allowed us to calculate G(intermolecular crosslinks) for three different dose rates, 0.150 Gy·s^{-1}, 0.013 Gy·s^{-1} and 0.0015 Gy·s^{-1}, at 0.15×10^{-7} mol·J^{-1}, 0.23×10^{-7} mol·J^{-1} and 0.62×10^{-7} mol·J^{-1}, respectively.

The observed yields of intermolecular crosslinks are significantly lower than the expected total yield of crosslinking. This fact, along with the observed dependence of G(intermolecular crosslinks) on the dose rate, indicates the importance of intramolecular recombination under our experimental conditions.

This process does not change the average molecular weight of the polymer but leads to changes in coil dimensions and flexibility (*cf.* refs. [40,47]). As expected, the lower dose rate favours an intermolecular recombination due to a lower probability for the presence of two or more radical sites on a single polymer chain in the steady state.

The existence of hydrophobic sites on the PVME chain that tend to associate in the inner part of the polymer coil leads to a kind of ordered structure, less flexible than expected for a random coil, *i.e.*, as mentioned above, to a very compact conformation of the PVME coils. This effect must slow down segmental diffusion and should lead to a reduced mobility of a radical located inside such a structure, nearly preventing this radical from intermolecular recombination. It seems probable that some of these single radicals trapped inside the coils undergo termination when, during further irradiation, another radical is formed within the same coil. This mechanism would enhance the yield of intramolecular at the expense of intermolecular crosslinking.

Discussion

Due to its compactness in aqueous solutions, PVME has properties that enables reactions to occur that may also be undergone by other polymers, but to a lesser extent. For example, there is now evidence that intramolecular crosslinking can be of much greater importance than intermolecular crosslinking even at very low radical steady-state concentrations. Thus conditions can be chosen easily that favour *e.g.* nanogel formation. This raises the question, whether compaction of other water-soluble polymers, *e.g.*, by the addition of salt or by lowering the temperature could be beneficial if nanogel formation is desired.

Irradiation at low aqueous polymer concentrations ($c < c^*$) does not result in the formation of macroscopic networks. Depending on the irradiation parameters (radiation dose, dose rate, polymer concentration, irradiation temperature) molecules with different structures can be obtained (long-chain branches, nanogels, microgel or microgel particles). Irradiation of the collapsed structure of PVME in diluted aqueous solutions above LCST leads to temperature-sensitive microgel particles [48]. These particles have a porous structures that serves as a template of emulsion polymerization of poly(pyrrole) to needle-like conductive polymer structures [49].

Increasing the dose rate (*e.g.* electron beam irradiation) increases the number of radicals at the polymer chain and changes the properties of the products. Irradiation of diluted aqueous solutions with pulsed electron beams (generation of a large number of radicals on each separate polymer chain in a short time) leads to the intramolecular combination of the produced radicals. In diluted homogeneous solutions (each macromolecule is separated) the formation of nanogels occurs [40,47,50,51].

The aim of the work was the pulsed electron beam irradiation of diluted aqueous PVME solutions in different concentrations to obtain internal crosslinked macromolecules (nanogels). These polymeric materials were characterized with respect to their molecular weight, dimension, viscosity, and temperature-sensitive behavior. Experiments at temperatures above the LCST were be performed to obtain temperature-sensitive microgels. Their size can be varied by irradiation at different polymer concentrations and different radiation doses. They are characterized with respect to their dimension and temperature-sensitivity.

Pulsed electron beam irradiation and measurements

Pulse irradiations were performed in a closed-loop flow system (Fig. 3) consisting of a solution reservoir, Tygon tubing, a peristaltic pump and a quartz irradiation cell (effective volume, $V = 0.7$ cm^3). Prior to and during the irradiation, polymer solution in the reservoir was being continuously saturated with Argon. The solution, flowing through the cell at a rate of 1 cm$^3 \cdot$s^{-1}, was pulse-irradiated with 6 MeV electrons generated by an ELU-6 linear accelerator (Eksma, Russia). Pulse frequency of 0.5 Hz and pulse duration of 3 μs were applied. The average dose absorbed per single pulse was determined by ferrocyanide dosimetry [52-54] to 0.96 kGy. The average dose for the whole solution volume was calculated based on the number of pulses applied as well as the known volume of the solution (500 cm^3) and the irradiation cell (0.7 cm^3).

The same irradiation facility was used for the synthesis of PVME microgels. Diluted aqueous PVME solutions ($c_p = 0.05, 0.1, 0.5$ g/l) were irradiated under phase-separated conditions. The temperature of the solution reservoir was adjusted to $T = 50\pm2$°C. Pulse frequency of 5 Hz and pulse duration of 3 μs were applied. The volume of the cuvette V was 1.0 ml.

The molecular weight M_w and the values of the hydrodynamic radius R_h were measured by the static and dynamic laser light scattering method based on a multi-angle Brookhaven Instruments setup consisting of a Lexel 95E argon ion laser (514.5 nm, typical output power 100±200 mW) and a BI-200SM goniometer. Measurements were performed using triple-distilled water as solvent.

By using static light scattering the angle and concentration dependence of the scattered light was measured at 25°C. ZIMM plot algorithm (see Eq. 4) was used to evaluate the scattering data.

$$\frac{K'c_B}{R(q)} = \frac{1}{M_w}\left(1 + \frac{1}{3}\left\langle r^2 \right\rangle_z^{1/2} q^2 \right) + 2A_2 c_B \quad (4)$$

where $K' = 4\pi^2 n^2/N_A \lambda_0^2 (\mathrm{d}n/\mathrm{d}c_B)^2$, the optical constant, c_B the polymer concentration, $R(q)$ the RAYLEIGH ratio, M_w the weight average of the molecular weight, $<r^2>_z^{1/2}$ the radius of gyration, q the scattering angle and A_2 the second virial coefficient.

The time correlation function of the scattering intensity, obtained by dynamic light scattering, was analyzed by using CONTIN fit.

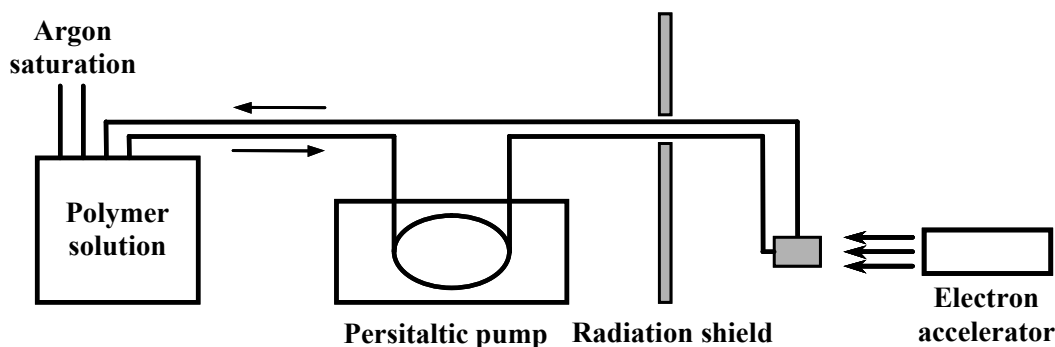$$\tau = \frac{1}{D \cdot q^2} \quad (5)$$

Fig. 3. Scheme of the irradiation setup (closed-loop system).

With the diffusion coefficients D the hydrodynamic radius R_h was calculated (Stokes-Einstein equation, eq. 5). For dynamic light scattering no extrapolation of $\vartheta \to 0$ and $c_p \to 0$ was done. An apparent hydrodynamic radius $R_{h,app}$ was determined.

$$R_h = \frac{k_B T}{6\pi\eta D} \qquad (6)$$

The samples were filtered through filters of 0.45 μm pore size directly before the measurement.

Molecular characterization

In dependence on the polymer concentration and the dose rate two different crosslinking reactions can be obtained: inter- and intramolecular crosslinking (see Fig. 4). If the numbers of radicals per single chain z_R is low ($z_R < 1$) the intermoleculare combination of the formed radicals is observed. Increasing the dose rate (dose D per time t) leads to increased amount of radicals per chain ($z_R > 1$). In diluted solutions these radicals crosslink intramolecularly. The additional crosslinks in these macromolecules lead to reduction of the dimension of the molecule. These kind of polymers are more resistant to degradation processes because a degradation of C–C main chain bonds do not reduce the molecular weight.

By using static light scattering in water the molecular weights of the PVME nanogels were determined in dependence on the radiation dose D and the polymer concentration c_p. The results are shown in Fig. 5.

a   **b**
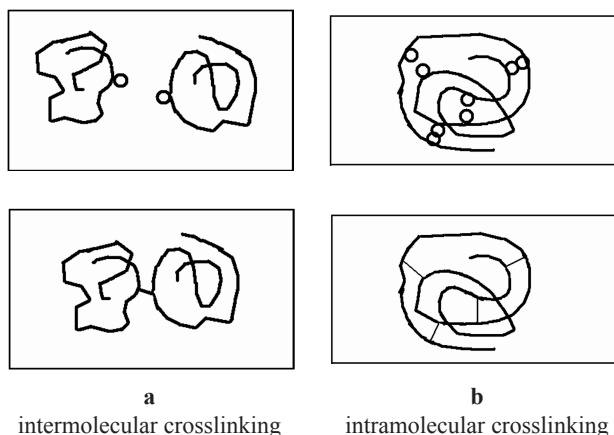intermolecular crosslinking   intramolecular crosslinking

Fig. 4. Scheme of the synthesis of PVME nanogels by radiation techniques. a) Single polymer chains with a low number of radicals crosslink intermolecularly. b) An increasing number of radicals per chain leads to an intramolecular crosslinking. Polymeric nanogels are formed.
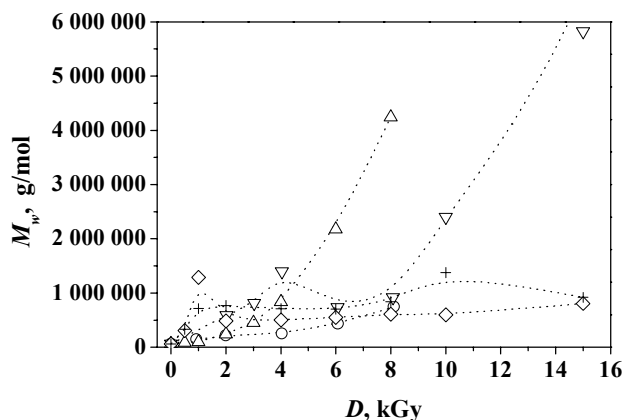
Fig. 5. Molecular weight M_w determined by static light scattering of the pulsed irradiated aqueous, de-oxygenated PVME solutions in dependence on the radiation dose D and the polymer concentration c_p (O – 10 mM, + – 17.5 mM, ◇ – 25 mM, ▽ – 50 mM, △ – 100 mM).

With increasing radiation dose the molecular weights of the PVME nanogels increase. A strong increasing M_w value was observed at high concentrations $c_p > 25$ mM.

The values of the radius of gyration $\langle r^2 \rangle_z^{1/2}$ were not evaluated because of the fact that at low polymer concentrations ($c_p < 25$ mM) the values are not realistic. The explanation of the reduction of the dimension of the internally crosslinked macromolecules was discussed by using the data of dynamic light scattering. The results are shown in Fig. 6.

At high polymer concentrations the value of $R_{h,app}$ increase with increasing radiation dose due to the
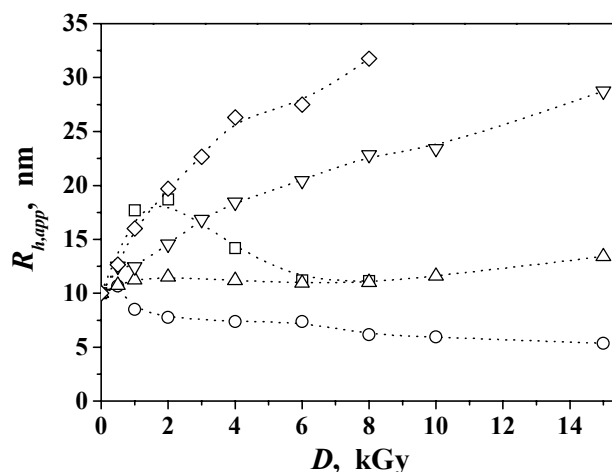
Fig. 6. Apparent hydrodynamic radius R_h ($\vartheta = 90°$) determined by dynamic light scattering of the pulsed irradiated aqueous, de-oxygenated PVME solutions versus the dependence of the radiation dose D and the polymer concentration c_p (□ – 10 mM, O – 17.5 mM, △ – 25 mM, ▽ – 50 mM, ◇ – 100 mM).

intermolecular crosslinking process. At $c_p = 25$ mM the radius is nearly constant at the initial value. At lower concentrations $R_{h,app}$ decreases with increasing D. The macromolecules crosslink intramolecularly and form nanogels.

PVME of high molecular weight

Vinyl ether monomers can not be polymerized in a radical way, only cationic. Cationic polymerized polymers (like in general vinyl ethers) have low molecular weights due to side reactions during the polymerization. Cation transfer reactions to already formed macromolecules lead to a long-chain branching of this polymer. The molecular weight of these polymers is relatively low ($M_w \approx 10^5$ g/mol) and the polydispersity is relatively high ($M_w/M_n > 2$).

That is why it is difficult to obtain vinyl ether polymers with high molecular weight. One possibility to increase the molecular weight of such polymer is the irradiation of their concentrated aqueous solutions with low doses below the gelation dose D_g. The crosslinking reaction of these polymers is intermolecularly and polymers with higher molecular weight are formed. However, they are long-chain branched.

Irradiation of this sample in the range of radiation dose $D = 0$-8 kGy leads to a small increasing of molecular weight and decreasing of dimensions (radius of gyration and hydrodynamic radius). In the range of very low doses the molecular weight and the dimension increase, again. Between 1 kGy and 6 kGy M_w ranges between 1,000,000 g/mol and 2,000,000 g/mol. Above 1 kGy the dimensions of the crosslinked PVME molecules decrease (Fig. 7).

Intermolecular crosslinking

In dependence on the radiation dose structural changes were obtained by different processes. The crosslinking and degradation reaction strongly depend on dose. At low dose values and at low polymer concentrations crosslinking is favored and main chain scission occurs rarely. Crosslinking of polymers by irradiation can occur on two different ways: intra- and intermolecular. The concentration of intermolecular crosslinks can be calculated using equation (eq. 3), where M_w^0 denotes the M_w of the non-irradiated polymer and c_p the polymer concentration of the irradiated aqueous solution. The calculated n_C values in dependence on the radiation dose are shown in Fig. 8.
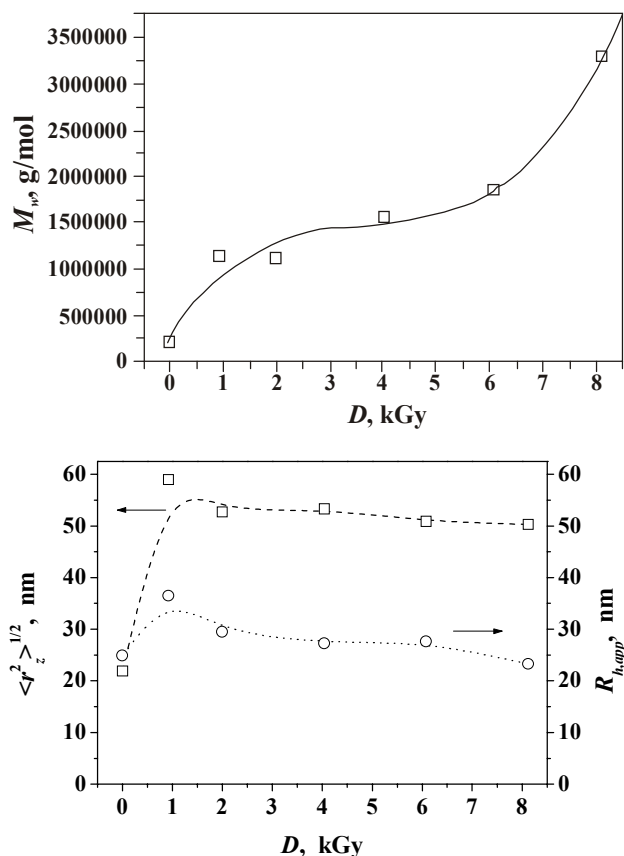

Fig. 7. Molecular weight M_w (Fig. 7a), radius of gyration $<r^2>_z^{1/2}$ (Fig. 7b), and apparent hydrodynamic radius R_h ($\vartheta = 90°$) (Fig. 7b) of the pulsed irradiated aqueous, deoxygenated PVME (γ-irradiated, *ca.* 30 kGy) solutions versus the radiation dose D.
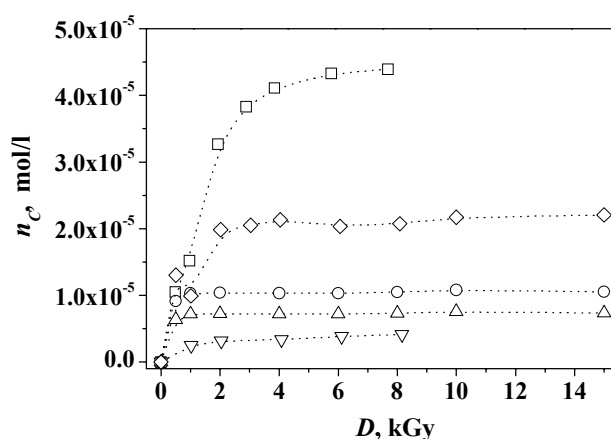

Fig. 8. Numbers of intermolecular crosslinks n_C calculated by using equation (3) in dependence on the radiation dose D and on the polymer concentration c_p (∇ – 10 mM, $\triangle$ – 17.5 mM, $\circ$ – 25 mM, $\diamond$ – 50 mM, $\square$ – 100 mM).

The value of the intermolecular crosslinks decreases with decreasing polymer concentration. At $c_p < 50$ mM and $D > 2$ kGy no significant changes in

these values could be observed. The crosslinking reaction occurs on the intramolecular way. Polymeric nanogels are formed.

Characterization of PVME microgels

In previous paper [48] it was found, that PVME molecules form globular particles in diluted aqueous solutions above the LCST (scheme of the synthesis is shown in Fig. 9). These phase-separated

aggregates have been crosslinked by electron beam irradiation to form temperature-sensitive microgels. The advantage of this method is the synthesis of such materials starting from the polymer and without the use of any additives (*e.g.* monomer, initiator, crosslinker, *etc.*). However, one can see that not all PVME molecules are crosslinked by the "static" method (irradiation of heated solutions in Petri dishes). Sol molecules remain in the microgel solution, which they have to be separated from [55].
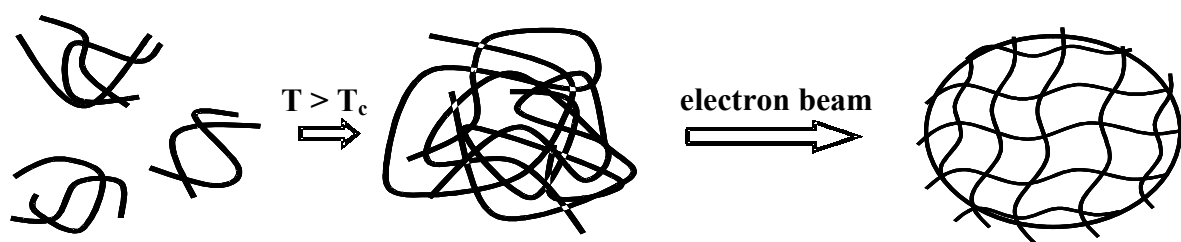

Fig. 9. Scheme of the synthesis of PVME microgels by radiation techniques. The associated polymer chains collapse at $T > T_c$ to globular aggregates [48]. This phase-separated structure of PVME is fixed by electron beam irradiation and temperature-sensitive microgels particles are formed.

Applying the closed-loop system under the same conditions ($c_p < c^*$, $T > T_{cr}$) can reduce the amount of sol molecules because of the irradiation in several steps (several loops). Experiments were performed at different polymer concentrations ($c_p = 0.05$-0.5 g/l) and different radiation doses ($D = 10$-80 kGy). Irradiation experiments at higher concentrations lead to the precipitation of the polymer.

The results of static light scattering measurement in the swollen ($T = 25°C$) and in the shrunken ($T = 50°C$) state are shown in Fig. 10.

Increasing the radiation dose D leads to decreasing of radii of gyration in the swollen state. The crosslinking density of the microgels increases and their swelling degree decreases. The radii in the shrunken state are nearly constant at $R_g = 120$ nm. The crosslinked phase-separated structure of PVME aggregates has always the same size (Fig. 11).

Dynamic light scattering measurements show the same tendency of the radii with increasing radiation dose. At low temperatures the value of the hydrodynamic radius decrease with increasing D. In the shrunken state the radii at low doses ($D < 25$ kGy) and at high doses ($D < 60$ kGy) are higher than the radii in medium range of dose. In former measurements it could be shown, that additional polymer in microgel solution collapse at the surface of these microgels (no separate aggregates are formed). At low doses still
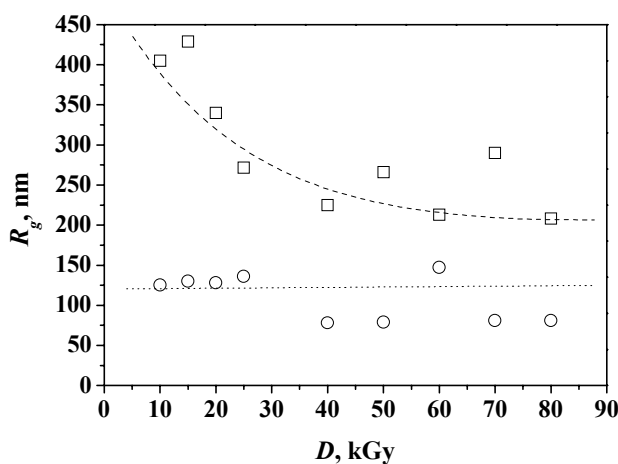

Fig. 10. Dose dependence of the radius of gyration R_g below ($\square$ – 25°C) and above T_{cr} ($\bigcirc$ – 50°C) of PVME microgels synthesized by pulsed electron beam irradiation (D/pulse = 850 Gy) of a diluted PVME solution ($c_p = 0.115$ g/l) at $T = 50\pm2°C$.

un-crosslinked sol molecules are in the microgel solution. These molecules collapse and increase the radius of the microgels observed at $T = 50°C$.

Conclusions

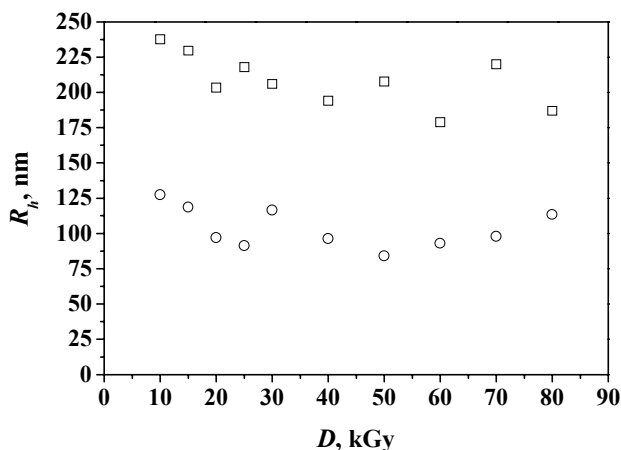It was shown, that various polymeric structures can be formed by applying pulsed electron beam ir-

Fig. 11. Dose dependence of the hydrodynamic radius R_h ($c_p \approx 10^{-3}$ g/l, $\vartheta = 20°$) below ($\square$ – 25°C) and above T_{cr} ($\circ$ – 50°C) of PVME. Nanogels synthesized by pulsed electron beam irradiation (D/pulse = 850 Gy) of a diluted PVME solution ($c_p = 0.115$ g/l) at $T = 50\pm2$°C.

radiation of aqueous de-oxygenated PVME solutions. Irradiation experiments at room temperature lead to the formation of PVME nanogels due to an intramolecular crosslinking reaction. At low radiation doses the molecular weight of PVME increases because of intermolecular crosslinking the relatively low M_w. With further increasing of the radiation dose at low polymer concentrations ($c_p < 25$ mM) no further increasing of molecular weight can be observed – intramolecular crosslinking reaction occurs. The hydrodynamic radii decrease with increasing dose. The dimension and the intrinsic viscosity of the internally crosslinked nanogels decrease.

Pulsed electron beam irradiation at temperatures above the LCST of PVME leads to the formation of temperature-sensitive microgel particles. Applying the closed-loop system reduces the amount of sol molecules. At low doses ($D < 25$ kGy) the sol content $s < 10\%$. For this purpose no further purification steps are necessary.

Acknowledgement

References

1. P. Molyneux, Water-Soluble Synthetic Polymers. Properties and Applications, CRC Press, Boca Raton, 1987.
2. H. Maeda, J. Polym. Sci. B, 1994, 32, 91.
3. H. Schafer-Soenen, R. Moerkerke, H. Berghmans, R. Koningsveld, K. Dusek, and K. Solc, Macromolecules, 1997, 30, 410.
4. F. Meeussen, Y. Bauwens, R. Moerkerke, E. Nies, and H. Berghmans, Polymer, 2000, 41, 3737.
5. O. Hirasa, S. Ito, A. Yamauchi, S. Fujishige, and H. Ochijo, in Polymer Gels, ed. D. De Rossi, Plenum Press, New York, 1991, p. 247.
6. B.G. Kabra, M.K. Akhtar, and S.H. Gehrke, Polymer, 1992, 33, 990.
7. J.Ed. Dusek, Responsive Gels: Volume Transitions, Springer, Berlin, 1993.
8. R. Moerkerke, F. Meeussen, R. Koningsveld, and H. Berghmans, Macromolecules, 1998, 31, 2223.
9. N.A. Peppas and J.J. Sahlin, Biomaterials, 1996, 17, 1553.
10. M.C. Bonferoni, S. Rossi, F. Ferrari, and C. Caramella, Pharm. Dev. Technol., 1999, 4, 45.
11. A.D. Woolfson, D.F. McCafferty, and G.P. Moss, Int. J. Pharm., 1998, 169, 83.
12. R. Kishi, H. Ichijo, and O. Hirasa, J. Intel. Mater. Syst. Struct., 1993, 4, 533.
13. H. Ichijo, R. Kishi, O. Hirasa, and Y. Takiguchi, Polym. Gels and Networks, 1994, 2, 315.
14. M. Hiraide and A. Morishima, Anal. Sci., 1997, 13, 829.
15. H. Ichijo, O. Hirasa, R. Kishi, M. Oowada, E. Kokufuta, and S. Ohno, Radiat. Phys. Chem., 1995, 185.
16. J.M. Rosiak and P. Ulanski, Radiat. Phys. Chem., 1999, 55, 139.
17. J.M. Rosiak, in Radiation Effects on Polymers, ed. R.C. Clough and S.W. Shalaby, Am. Chem. Soc., Washington, 1991, p. 271.

18. J.M. Rosiak, J. Controlled Release, 1994, 31, 9.

19. X.D. Liu, R.M. Briber, and B.J. Bauer, J. Polym. Sci. B: Polym. Phys., 1994, 32, 811.

20. S. Sabharval, H. Mohan, Y.K. Bhardwaj, and A.B. Majali, J. Chem. Soc. Farad. Trans., 1996, 92, 4401.

21. S. Sabharval, H. Mohan, Y.K. Bhardwaj, and A.B. Majali, Radiat. Phys. Chem., 1999, 54, 643.

22. I. Janik, P. Ulanski, and J.M. Rosiak, Nucl. Instr. Meth. Phys. Res. B, 1999, 151, 318.

23. I. Janik, P. Ulanski, J. M. Rosiak, and C. von Sonntag, submitted to J. Chem. Soc. Perkin Trans 2.

24. C. von Sonntag and H.-P. Schuchmann, Methods Enzymol., 1994, 233, 3.

25. G.V. Buxton and C.R. Stuart, J. Chem. Soc. Faraday Trans., 1995, 91, 279.

26. D. Veltwisch, E. Janata, and K.-D. Asmus, J. Chem. Soc. Perkin Trans. II, 1980, 146.

27. F. Lipari and S.J. Swarin, J. Chromatogr., 1982, 247, 297.

28. A.O. Allen, C.J. Hochanadel, J.A. Ghormley, and T.W. Davis, J. Phys. Chem., 1952, 56, 575.

29. P. Dowideit and C. von Sonntag, Environ. Sci. Technol., 1998, 32, 1112.

30. M.N. Schuchmann and C. von Sonntag, Z. Naturforsch., 1987, 42b, 495.

31. C. Nese, M.N. Schuchmann, S. Steenken, and C. von Sonntag, J. Chem. Soc. Perkin Trans. 2, 1995, 1037.

32. G.V. Buxton, C.L. Greenstock, W.P. Helman, and A.B. Ross, J. Phys. Chem. Ref. Data, 1988, 17, 513.

33. H.-P. Schuchmann and C. von Sonntag, Radiat. Phys. Chem., 1988, 32, 149.

34. C. von Sonntag, E. Bothe, P. Ulanski, and A. Adhikary, Radiat. Phys. Chem., 1999, 55, 599.

35. J. Eibenberger, D. Schulte-Frohlinde, and S. Steenken, J. Phys. Chem., 1980, 84, 704.

36. I. A. Raap and U. Gröllmann, Macromol. Chem., 1983, 184, 123.

37. P. Ulanski, E. Bothe, J.M. Rosiak, and C. von Sonntag, Makromol. Chem., 1994, 195, 1443.

38. P. Ulanski, Zainuddin, and J.M. Rosiak, Radiat. Phys. Chem., 1995, 46, 917.

39. P. Ulanski, E. Bothe, K. Hildenbrand, J.M. Rosiak, and C. von Sonntag, J. Chem. Soc. Perkin Trans. 2, 1996, 13.

40. P. Ulanski, I. Janik, and J.M. Rosiak, Radiat. Phys. Chem., 1998, 52, 289.

41. P. Ulanski, E. Bothe, and C. von Sonntag, Nucl. Instr. Meth. Phys. Res. B, 1999, 151, 350.

42. P. Ulanski, E. Bothe, K. Hildenbrand, and C. von Sonntag, Chem. Eur. J., 2000, 6(21), 3922

43. P. Ulanski, E. Bothe, K. Hildenbrand, C. von Sonntag, and J.M. Rosiak, Nukleonika, 1997, 42, 425.

44. B.G. Ershov, Russ. Chem. Rev., 1998, 67, 315.

45. A. Charlesby, Atomic Radiation and Polymers, Pergamon Press, Oxford, 1960.

46. W. Schnabel, Polymer Degradation. Principles and Practical Applications, Hanser, München, 1981.

47. P. Ulanski and J.M. Rosiak, Nucl. Instr. Meth. Phys. Res. B, 1999, 151, 356.

48. Arndt KF, Schmidt T, Reichelt R., Polymer 2001; 42, 6785.

49. Pich A., Lu Y., Adler H.J.P, Schmidt T., Arndt K.F., Polymer 2002, 43, 5723.

50. UlaDski P., KadBubowski S., Rosiak J.M., Rad. Phys. Chem. 2002, 63, 533.

51. KadBubowski S., Grobelny J., Olejniczak W., Cichomski M., UlaDski P., Macromolecules , 2003, 36, 2484.

52. Rabani J., Matheson M.S., J. Phys. Chem. 1966, 70, 761.

53. Broszkiewicz R., Chemical Methods of Dosimetry of Ionising Radiation, Warsaw: WNT, 1971.

54. Schuler R.H., Hartzell A.L., Behar B., J. Chem. Phys., 1981, 85, 192.

55. Schmidt T., Querner C., Arndt K.F., Nucl. Instrum. Methods. Phys. Res. B, 2003, 208, 331.